

Diagnosing Relativistic Electron Distributions in the Van Allen Radiation Belts

S. Killey^[1], I.J. Rae^[1], S. Chakraborty^[1], A.W. Smith^[1], S.N. Bentley^[1], M. R. Bakrania^[2], R. Wainwright^[1], C.E.J. Watt^[1], and J. K. Sandhu^[1]

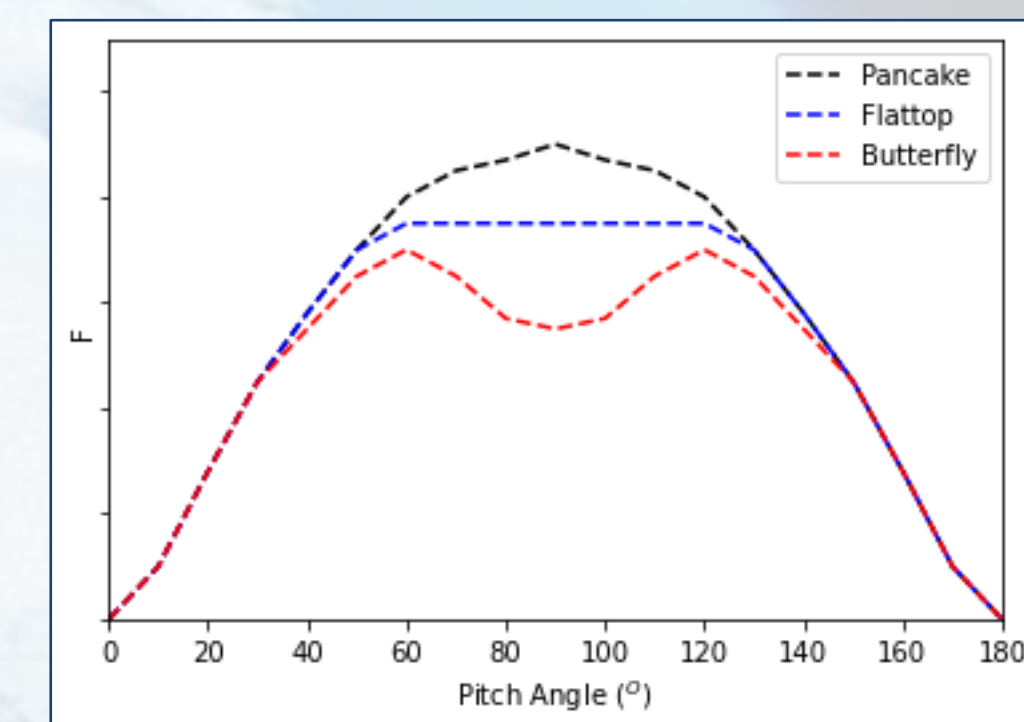
^[1] Northumbria University, Newcastle Upon Tyne, NE1 8ST
^[2] Mullard Space Science Laboratory, UCL, Dorking, RH5 6NT

Relativistic Electron Pitch Angle Distributions:

The Van Allen radiation belts are plasma regions that surround the Earth and are populated by energetic particles. The radiation belts are highly dynamic, meaning that energetic particle behaviour in the belts is difficult to diagnose. Relativistic electron (energies $> 10^6$ eV) behaviour in the belts is driven by a multitude of physical processes that occur at different energies and pitch angles (Chakraborty et al, 2022). Energetic particles in the radiation belts travel along the Earth's magnetic field in a helical motion (gyromotion), therefore pitch angle refers to the angle between the magnetic field and the velocity vector of the energetic particle. These physical processes result in differently shaped energy dependent pitch-angle distributions (PADs). Pitch-angle distribution are vital to understand plasma conditions (Bakrania et al, 2020).

Table 1. Typical types of PADs and the physical process that causes them (Chakraborty et al, 2022). A description of their shape is also given.

| Shape | Description | Physical Process |
|-------------|--|---|
| ✦ Flattop | plateau of flux across a range of pitch angles centred on 90° . | wave-particle interactions |
| ✦ Butterfly | decrease in flux at 90° . | wave-particle interactions with chorus and magnetosonic waves |
| ✦ Pancake | a peak centred on 90° . | wave-particle interactions, radial diffusion |



This study applies a compilation of unsupervised techniques to Van Allen Probe REPT data in order to classify observations with similarly shaped PADs (Killey et al, 2023).

7 Years Van Allen Probe REPT Data:

- ✦ Resolution of the order of 10s.
- ✦ 17 different pitch angles.
- ✦ 12 different energies between 1 – 20 MeV.
- ✦ Normalised with respect to the maximum value of each observation.
- ✦ A 20:20:60 data split was selected for the training, validation and testing sets respectively.

Dimension Reduction, Reproducibility and Classification

- ✦ Apply a random seed of 1 to account for reproducibility.
- ✦ Compress the 204 dimensional REPT data to 102 dimensions using an Autoencoder.
- ✦ Further compress the data to 3D using principal component analysis.
- ✦ Predict the number of classifications in 3D REPT data using a mean shift algorithm.
- ✦ Apply this number of classifications to a K-means clustering algorithm.

Clusters:

The amalgamation of unsupervised learning techniques determined that in the 3D representation of REPT data, there were 6 different clusters, which are shown in Figure 1. To account for ambiguity of classifications at the boundaries of the clusters, a 95% confidence interval was applied.

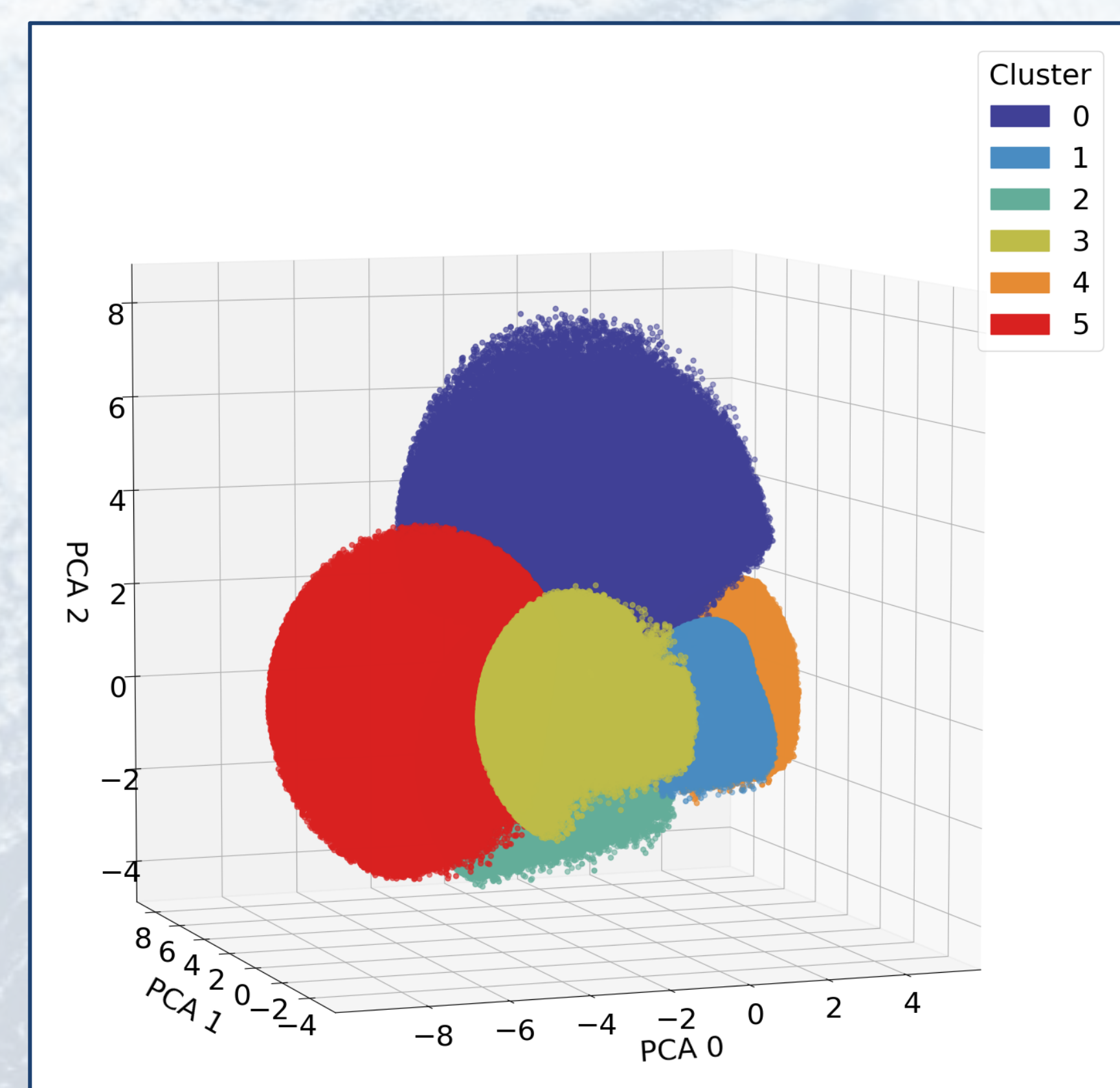


Figure 1: 3D representation of 7 years of Van Allen Probe REPT data, partitioned into 6 different K-means clusters.

Pitch Angle Distribution Shapes:

By plotting the mean normalised PAD of each cluster across all energies, as shown in Figure 2, we determined that each cluster has a differently shaped PAD.

- ✦ **Cluster 0** (Figure 2a): flattop.
- ✦ **Cluster 1** (Figure 2b): pancake.
- ✦ **Cluster 2** (Figure 2c): butterfly and a flattop.
- ✦ **Cluster 3** (Figure 2d): narrow pancake.
- ✦ **Cluster 4** (Figure 2e): weak butterfly.
- ✦ **Cluster 5** (Figure 2f): weak flattop.

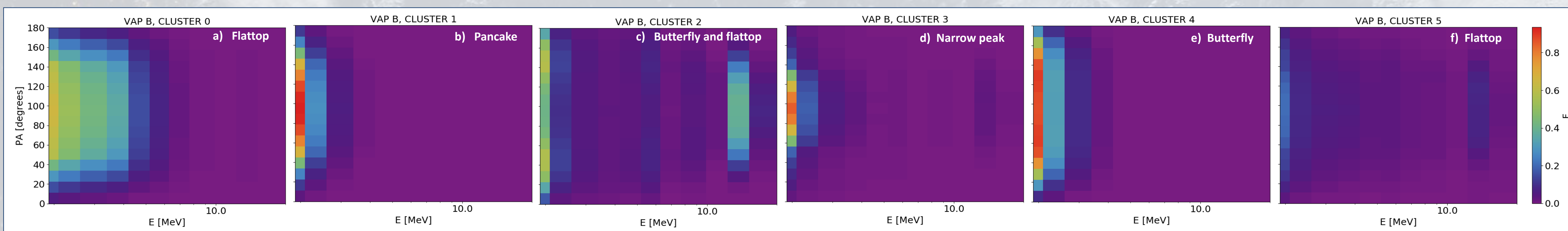


Figure 2: The PADs of each identified cluster across all energies. The colour-bar represents the mean normalised flux. The shapes of the PADs of each cluster are slightly different

- ✦ Clusters 0 – 4 displayed the same distribution shapes in the median PADs, as shown in Figure 3.
- ✦ Cluster 5 (Figure 3f) displayed a net median flux of 0, revealing a cluster containing only low counts and noisy signatures.
- ✦ At lower energies, the remaining 5 clusters have distribution shapes as expected from literature- either flattop, butterfly or pancake (e.g. Chakraborty et al. 2022).

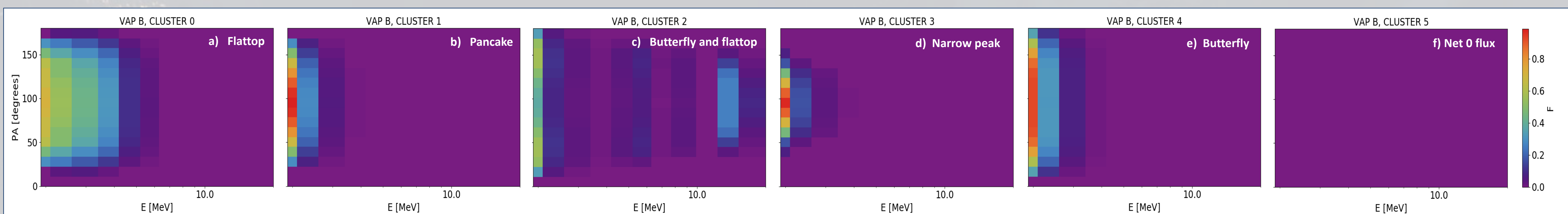


Figure 3: The median PADs of each identified cluster across all energies..

Conclusions:

- ✦ Unsupervised machine learning techniques were applied to compress and classify all 7 years of REPT data into 6 different clusters.
- ✦ All clusters have differently shaped mean energy dependent PADs, where at low energies have either a flattop, butterfly or pancake shape as expected.
- ✦ Median PADs revealed 5 clusters with the same shaped PADs as their mean PADs and 1 cluster that contained a net flux of 0.
- ✦ Cluster 5 only contained low counts and noisy data, suggesting that this method has also inadvertently denoised the REPT data.

Acknowledgements:

SK is indebted to Northumbria University and STFC grant 2597922 for PhD studentship support. IJR, SC, JKS are funded in part by STFC grants ST/V006320/1, and NERC grants NE/V002554/2 and NE/P017185/2. RW was supported by a Royal Astronomical Society Summer Studentship. AWS was supported by NERC Independent Research Fellowship NE/W009129/1. MRB was supported by a UCL Impact Studentship, joint funded by the ESA NPI programme. CEJW is supported by NERC grant NE/V002759/1 and STFC grant ST/W000369/1.

References:

Bakrania et al (2020), Using dimensionality reduction and clustering techniques to classify space plasma regimes, *Frontiers in Astronomy and Space Sciences*
Chakraborty et al (2022), Statistical investigation on equatorial pitch angle distribution of energetic electrons in earth's outer radiation belt during cme- and cir-driven storms, *Frontiers in Astronomy and Space Sciences*
Killey et al (2023), Using Machine Learning to Diagnose Relativistic Electron Distributions in the Van Allen Radiation Belts. *ESS Open Archive*, preprint